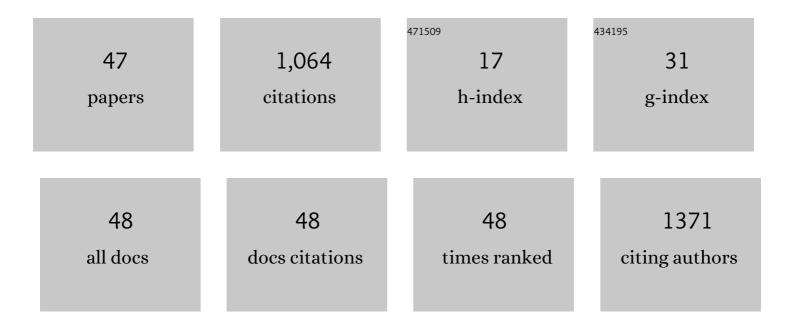
Kei Nishikawa

List of Publications by Year in descending order

Source: https://exaly.com/author-pdf/6089367/publications.pdf Version: 2024-02-01



KEI NICHIKANAA

#	Article	IF	CITATIONS
1	Effects of Phase Change and Cu Doping on the Li Storage Properties of Rutile TiO ₂ . Electrochemistry, 2022, 90, 037002-037002.	1.4	12
2	Effects of Carbonate Solvents and Lithium Salts in High-Concentration Electrolytes on Lithium Anode. Journal of the Electrochemical Society, 2022, 169, 060548.	2.9	5
3	In Situ Observation of Cu ²⁺ Concentration Profile During Cu Dissolution in Magnetic Field. Journal of the Electrochemical Society, 2021, 168, 031507.	2.9	5
4	Characterization of Electrodeposited Li Metal by Cryo-Scanning Transmission Electron Microscopy/Electron Energy Loss Spectroscopy. Journal of Physical Chemistry Letters, 2021, 12, 3922-3927.	4.6	15
5	Improvement of Preparation Scheme for Microelectrode and Single Particle Electrochemical Measurements of LiCoO2 Interfaces Under Absence / Presence Chemical Additives. ECS Meeting Abstracts, 2021, MA2021-01, 22-22.	0.0	Ο
6	Metallographic Structure Changes in Lanthanum Silicide/Silicon Nanocomposite Electrodes during Lithiation and Delithiation: Implications for Battery Applications. ACS Applied Nano Materials, 2021, 4, 8473-8481.	5.0	8
7	<i>In situ</i> interferometry study of ionic mass transfer phenomenon during the electrodeposition and dissolution of Li metal in solvate ionic liquids. Journal of Materials Chemistry A, 2021, 9, 14700-14709.	10.3	9
8	Lithiation/Delithiation Properties of Lithium Silicide Electrodes in Ionic-Liquid Electrolytes. ACS Applied Materials & Interfaces, 2021, 13, 3816-3824.	8.0	15
9	3D Structural Transition of the Electrodeposited and Electrochemically Dissolved Li Metal onto an Ultramicroelectrode. Journal of Physical Chemistry C, 2020, 124, 22019-22024.	3.1	8
10	Precise Analysis of Resistance Components and Estimation of Number of Particles in Li-Ion Battery Electrode Sheets Using LiCoO ₂ Single-Particle Electrochemical Properties. Journal of Physical Chemistry C, 2020, 124, 16758-16762.	3.1	7
11	Reaction Behavior of a Silicide Electrode with Lithium in an Ionic-Liquid Electrolyte. ACS Omega, 2020, 5, 22631-22636.	3.5	12
12	Analysis of the Li Distribution in Si-Based Negative Electrodes for Lithium-Ion Batteries by Soft X-ray Emission Spectroscopy. ACS Applied Energy Materials, 2020, 3, 8619-8626.	5.1	18
13	Macroporous Mn3O4 microspheres as a conversion-type anode material morphology for Li-ion batteries. Journal of Solid State Electrochemistry, 2020, 24, 1283-1290.	2.5	7
14	Conversion Reaction in the Binder-Free Anode for Fast-Charging Li-Ion Batteries Based on WO ₃ Nanorods. ACS Applied Energy Materials, 2020, 3, 6700-6708.	5.1	20
15	In Situ Measurement of Al ³⁺ Concentration Profile during Al Anodization using Digital Holographic Interferometric Microscope. Journal of the Electrochemical Society, 2020, 167, 062501.	2.9	7
16	Asymmetry in the Solvation–Desolvation Resistance for Li Metal Batteries. Analytical Chemistry, 2020, 92, 3499-3502.	6.5	13
17	Electrochemical Lithiation and Delithiation Properties of FeSi ₂ /Si Composite Electrodes in Ionic-Liquid Electrolytes. Electrochemistry, 2020, 88, 548-554.	1.4	10
18	Deterioration Analysis of Lithium Metal Anode in Full Cell during Long-Term Cycles. Journal of the Electrochemical Society, 2019, 166, A2618-A2628.	2.9	13

Kei Nishikawa

#	Article	IF	CITATIONS
19	Effect of Frequency-Dependent Fresnel Factor on the Vibrational Sum Frequency Generation Spectra for Liquid/Solid Interfaces. Journal of Physical Chemistry C, 2019, 123, 15665-15673.	3.1	25
20	Surface State Change of Lithium Metal Anode in Full Cell during Long Term Cycles. Electrochemistry, 2019, 87, 84-88.	1.4	15
21	Holographic interferometric microscopy for measuring Cu2+ concentration profile during Cu electrodeposition in a magnetic field. Electrochimica Acta, 2019, 297, 1104-1108.	5.2	22
22	Electrodeposition of Zn from 1â€ʻallylâ€ʻ3â€ʻmethylimidazolium bromide containing ZnBr2. Journal of Electroanalytical Chemistry, 2019, 832, 467-474.	3.8	7
23	Degradation Analysis of LiNi _{0.8} Co _{0.15} Al _{0.05} O ₂ for Cathode Material of Lithium-Ion Battery Using Single-Particle Measurement. ACS Applied Energy Materials, 2018, 1, 4536-4544.	5.1	31
24	Intrinsic electrochemical characteristics of one LiNi0.5Mn1.5O4 spinel particle. Journal of Electroanalytical Chemistry, 2017, 799, 468-472.	3.8	20
25	Intrinsic Electrochemical Characteristics in the Individual Needle-like LiCoO ₂ Crystals Synthesized by Flux Growth. Electrochemistry, 2017, 85, 72-76.	1.4	8
26	In-situ observation of volume expansion behavior of a silicon particle in various electrolytes. Journal of Power Sources, 2016, 302, 46-52.	7.8	27
27	Flux growth of hexagonal cylindrical LiCoO ₂ crystals surrounded by Li-ion conducting preferential facets and their electrochemical properties studied by single-particle measurements. Journal of Materials Chemistry A, 2015, 3, 17016-17021.	10.3	20
28	Optical observation of Li dendrite growth in ionic liquid. Electrochimica Acta, 2013, 100, 333-341.	5.2	85
29	In-situ observation of one silicon particle during the first charging. Journal of Power Sources, 2013, 243, 630-634.	7.8	36
30	Electrodeposition of metals in microgravity conditions. Electrochimica Acta, 2013, 100, 342-349.	5.2	11
31	Evolution of the Morphology of Electrodeposited Copper at the Early Stage of Dendritic Growth. Journal of the Electrochemical Society, 2013, 160, D183-D187.	2.9	13
32	Morphological Variation of Electrodeposited Li in Ionic Liquid. ECS Transactions, 2012, 41, 3-10.	0.5	14
33	Li dendrite growth and Li+ ionic mass transfer phenomenon. Journal of Electroanalytical Chemistry, 2011, 661, 84-89.	3.8	101
34	Electrodeposition experiments in microgravity conditions. Journal of Physics: Conference Series, 2011, 327, 012045.	0.4	5
35	In situ concentration measurements around the transition between two dendritic growth regimes. Electrochimica Acta, 2011, 56, 5464-5471.	5.2	9
36	In Situ Observation of Dendrite Growth of Electrodeposited Li Metal. Journal of the Electrochemical Society, 2010, 157, A1212.	2.9	123

Kei Nishikawa

#	Article	IF	CITATIONS
37	Three-dimensionally ordered macroporous Ni–Sn anode for lithium batteries. Journal of Power Sources, 2009, 189, 726-729.	7.8	72
38	Numerical Analysis of Ionic Mass Transfer Phenomena Accompanying Electrochemical Reactions in PC and Ionic Liquid. Electrochemistry, 2009, 77, 601-603.	1.4	2
39	Diffusivity Measurement of LiPF6, LiTFSI, LiBF4 in PC. ECS Transactions, 2008, 6, 1-14.	0.5	38
40	Measurement of Concentration Profiles during Electrodeposition of Li Metal from LiPF[sub 6]-PC Electrolyte Solution. Journal of the Electrochemical Society, 2007, 154, A943.	2.9	35
41	Measurement of concentration profile during charging of Li battery anode materials in LiClO4-PC electrolyte. Electrochimica Acta, 2007, 53, 218-223.	5.2	8
42	In situ measurement of lithium mass transfer during charging and discharging of a Ni–Sn alloy electrode. Journal of Power Sources, 2007, 174, 668-672.	7.8	16
43	Numerical simulation of transient natural convection induced by electrochemical reactions confined between vertical plane Cu electrodes. Electrochimica Acta, 2007, 53, 257-264.	5.2	24
44	Measurement of LiClO[sub 4] Diffusion Coefficient in Propylene Carbonate by Moire̕Pattern. Journal of the Electrochemical Society, 2006, 153, A830.	2.9	29
45	Ionic mass transfer during electrochemical dissolution of Li metal in PC electrolyte solution. Journal of Electroanalytical Chemistry, 2005, 584, 63-69.	3.8	20
46	Transient natural convection induced by electrodeposition of Li + ions onto a lithium metal vertical cathode in propylene carbonate. Journal of Solid State Electrochemistry, 2004, 8, 174-181.	2.5	17
47	Measurement of concentration boundary layer thickness development during lithium electrodeposition onto a lithium metal cathode in propylene carbonate. Journal of Electroanalytical Chemistry, 2003, 559, 175-183	3.8	47